Article

Sulfur Radical Cation–Peptide Bond Complex in the One-Electron Oxidation of *S*-Methylglutathione

Krzysztof Bobrowski, Gordon L. Hug, Dariusz Pogocki, Bronislaw Marciniak, and Christian Schneich

J. Am. Chem. Soc., **2007**, 129 (29), 9236-9245• DOI: 10.1021/ja072301f • Publication Date (Web): 29 June 2007

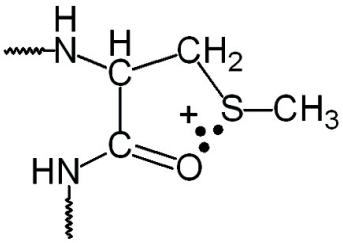

More About This Article

Additional resources and features associated with this article are available within the HTML version:

- Supporting Information
- Links to the 3 articles that cite this article, as of the time of this article download
- Access to high resolution figures
- Links to articles and content related to this article
- Copyright permission to reproduce figures and/or text from this article

View the Full Text HTML

J|A|C|S
ARTICLES
Published on Web 06/29/2007

Sulfur Radical Cation−Peptide Bond Complex in the One-Electron Oxidation of *S*-Methylglutathione

Krzysztof Bobrowski,[†] Gordon L. Hug,*[,‡,§,#] Dariusz Pogocki,[†,||] Bronislaw Marciniak,[§] and Christian Schöneich[⊥]

Contribution from the Institute of Nuclear Chemistry and Technology, 03-195 Warsaw, Poland, Radiation Laboratory, University of Notre Dame, Notre Dame, Indiana 46556, Faculty of Chemistry, A. Mickiewicz University, 60-780 Poznan, Poland, Faculty of Chemistry, Rzeszow University of Technology, 35-959 Rzeszow, Poland, Department of Pharmaceutical Chemistry, University of Kansas, Lawrence, Kansas 66047

Received April 2, 2007; E-mail: hug.1@nd.edu

Abstract: Neighboring group participation was investigated in the •OH-induced oxidation of *S*-methylglutathione in aqueous solutions. Nanosecond pulse radiolysis was used to obtain the spectra of the reaction intermediates and their kinetics. Depending on the pH, and the concentration of *S*-methylglutathione, pulse irradiation leads to different transients. The transients observed were an intramolecularly bonded $[>S\therefore NH_2]^+$ intermediate, intermolecularly S∴S-bonded radical cation, α-(alkylthio)alkyl radicals, α-amino-alkyl-type radical, and an intramolecularly $(S\therefore O)^+$-bonded intermediate. The latter radical is of particular note in that it supports recent observations of sulfur radical cations complexed with the oxygen atoms of peptide bonds and thus has biological and medical implications. This $(S\therefore O)^+$-bonded intermediate had an absorption maximum at 390 nm, and we estimated its formation rate to be $\geq 6 \times 10^7$ s^{-1}. It is in equilibrium with the intermolecularly S∴S-bonded radical cation, and they decay together on the time scale of a few hundred microseconds. The S∴S-bonded radical cation is formed from the monomeric sulfur radical cation ($>S^{\bullet+}$) and an unoxidized *S*-methylglutathione molecule with the rate constant of 1.0×10^9 M^{-1} s^{-1}. The short-lived $[>S\therefore NH_2]^+$ intermediate is a precursor of decarboxylation, absorbs at ∼ 390 nm, and decays on the time scale of hundreds of nanoseconds. Additional insight into the details of the association of sulfur radical cations with the oxygen atoms of the peptide bonds was gained by comparing the behavior of the *S*-methylglutathione ($S\therefore O^+$-bonded five-membered ring) with the peptide γ-Glu-Met-Gly ($S\therefore O^+$-bonded six-membered ring). Conclusions from experimental observations were supported by molecular modeling calculations.

Introduction

Neighboring group participation is an important concept for understanding how the oxidation of organic sulfides is controlled.[1,2] This concept refers to how neighboring groups can direct the attack of an oxidizing agent and can moderate the fate of any damaged sites. In one-electron oxidation of organic sulfides, sulfur-centered radical cations are formed, and they generally disappear by deprotonation unless neighboring groups are present. These neighboring groups can provide a lone pair of electrons which can be shared with the sulfur radical cation center, $>S^{\bullet+}$, forming a three-electron-bonded species which effectively stabilizes the radical.[1,3,4] The same applies to the •OH-induced oxidation of organic sulfides where normally the •OH radicals directly attack the sulfur, forming hydroxysulfuranyl radicals, but their subsequent reactions are strongly influenced by the presence of neighboring groups. These secondary reactions involving the interaction of the sulfur-centered radical cations and hydroxysulfuranyl radicals with hydroxyl, amide, amino, and carboxyl moieties were observed in simple model compounds like alcohols,[5−9] amides,[5] amines,[10] carboxylic acids,[9,11−13] and aminoacids.[14−19]

[†] Institute of Nuclear Chemistry and Technology.
[‡] University of Notre Dame.
[§] A. Mickiewicz University.
[||] Rzeszow University of Technology.
[⊥] University of Kansas.
[#] Fulbright Scholar in the Faculty of Chemistry, A. Mickiewicz University, 60-780 Poznan, Poland. Permanent address: Radiation Laboratory, University of Notre Dame, Notre Dame, Indiana.

(1) Glass, R. S. Neighbouring group participation: General principles and application to sulfur-centered reactive species. In *Sulfur-Centered Reactive Intermediates in Chemistry and Biology*; Chatgilialoglu, C., Asmus, K.-D., Eds.; Plenum Press: New York, 1990; Vol. 97, pp 213−226.
(2) Glass, R. S.; Hojjatie, M.; Petsom, A.; Wilson, G. S.; Göbl, M.; Mahling, S.; Asmus, K.-D. *Phosphorus Sulfur* **1985**, *23*, 143−168.
(3) Asmus, K.-D. Heteroatom-centered free radicals. Some selected contributions by radiation chemistry. In *Radiation Chemistry: Present Status and Future Prospects*; Jonah, C., Rao, B. S. M., Eds.; Elsevier Science: Amsterdam, 2001; pp 341−393.
(4) Asmus, K.-D.; Bonifacic, M. Sulfur-centered reactive intermediates as studied by radiation chemical and complementary techniques. In *S-Centered Radicals*; Alfassi, Z. B., Ed.; John Wiley & Sons Ltd.: Chichester, 1999; pp 141−191.
(5) Bobrowski, K.; Hug, G. L.; Marciniak, B.; Schöneich, C.; Wiœniowski, P. *Res. Chem. Intermed.* **1999**, *25*, 285−297.
(6) Bobrowski, K.; Hug, G. L.; Marciniak, B.; Miller, B. L.; Schöneich, C. *J. Am. Chem. Soc.* **1997**, *119*, 8000−8011.
(7) Schöneich, C.; Bobrowski, K. *J. Am. Chem. Soc.* **1993**, *115*, 6538−6547.

10.1021/ja072301f CCC: $37.00

Such neighboring group effects can occur in more complex molecules, sometimes over quite long distances, as was demonstrated for •OH-induced oxidations of a series of dipeptides, each containing a C-terminal methionine (Met). The N-terminal residues in this series were methionyl (Met),[20,21] glycyl (Gly), alanyl (Ala), valyl (Val), leucyl (Leu),[22] γ-glutamic acid (γ-Glu),[22,23] seryl (Ser), and threonyl (Thr) residues.[24,25] A key step in the proposed oxidation mechanism might involve an intramolecular proton transfer to the initially formed methionyl hydroxysulfuranyl radical (**I**) from the neighboring, albeit remote, protonated N-terminal amino group. This process leads to the formation of a three-electron bonded $[>S\therefore NH_2]^+$-peptide intermediate (**II**) (reaction 1).

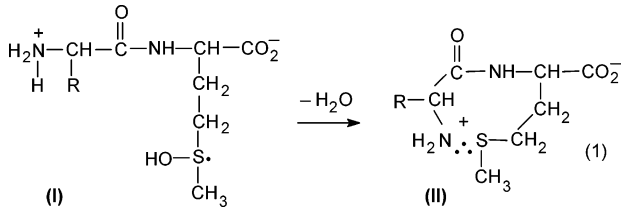

For the specific case of N-terminal γ-Glu, species **II** decomposes into an α-amino radical and CO_2,[23] whereas N-terminated Ser and Thr yield formaldehyde and acetaldehyde, respectively.[25] In competition with the formation of **II**, the hydroxysulfuranyl radical **I** may decompose into the sulfur radical cation, which subsequently disappears through C-terminal decarboxylation (when the sulfur radical is on the C-terminal residue), deprotonation, or formation of a sulfur−sulfur three-electron bonded dimeric species. The relative ratio of **II** and **I** is controlled by the nature of the *S*-alkyl substituent.

The *S*-methylglutathione, investigated in the current work, is a tripeptide with a potentially larger scope for neighboring group participation than the above dipeptides. There are many different functional groups within the same molecule, and in particular, the sulfur-containing side chain is an interior residue. This latter feature has consequences with regard to the interaction between the site of the sulfur radical cation and the C-terminal carboxyl group. Because a weaker interaction is expected between these two moieties, it opens the possibility for the interaction of the sulfur-centered radical cations with oxygens in the peptide backbone. *S*-Methylglutathione also represents a particularly good model system for studying N-terminal decarboxylation induced through the initial reaction of •OH at the central *S*-methyl-Cys residue. This process resulted in significantly different yields of decarboxylation upon variation of the peptide concentration, pH, and the character of the alkyl substituent at the thioether functionality.[26]

In the current work, we have established a qualitative and quantitative picture of the reaction mechanism as a function of pH and the concentration of the peptide using nanosecond pulse radiolysis. These studies provide further evidence for an intermediate formed through the intramolecular association between a sulfur radical cation and a peptide-bond oxygen,[27] and related complexes.[28] Additional insight into the details of this new oxidation mechanism was gained by comparing the behavior of the *S*-methylglutathione (γ-Glu-*S*-Me-Cys-Gly) with the peptide γ-Glu-Met-Gly. This comparison has the following advantages. Methionine is the homologue of *S*-methylcysteine (*S*-Me-Cys), and any contrasting behavior of these two residues will provide insight into the kinetic and thermodynamic preference for six- versus five-membered ring configurations, respectively, in the formation of intramolecularly $(S\therefore O)^+$-bonded species.

S-alkylglutathiones are naturally occurring oligopeptides. For instance, *S*-methylglutathione is an inhibitor of the glyoxalase cycle[29] and protects the glutathione transferase from inactivation.[30] *S*-alkylglutathiones act as selective ligands of brain ionotropic glutamate receptors.[31] They are also common products from the metabolism of alkyl halides by glutathione *S*-transferases in human erythrocytes.[32,33] These studies are of relevance to interactions between remote sites in proteins and any site under direct oxidative attack. These oligopeptides can serve as primary models for peptide molecules of biological importance where, for example, higher-order structures may bring functional groups into close proximity to the thioether group.

Experimental Section

Materials. *S*-Methylglutathione (*S*-MeGlu) was purchased from Sigma. See Chart 1 for the structures of the peptides used in this work. *S*-MeGlu (batch no. 35H7862) appeared to contain iodide contamination that we removed by recrystallizing *S*-MeGlu from a mixture of water and acetone before use. The iodide impurity could have caused serious interference with monitoring transient absorptions in the visible region of the spectrum. The "crystals" were amorphous, but the *S*-MeGlu

(8) Mahling, S.; Asmus, K.-D.; Glass, R. S.; Hojjatie, M.; Wilson, G. S. *J. Org. Chem.* **1987**, *52*, 3717−3724.
(9) Glass, R. S.; Hojjatie, M.; Wilson, G. S.; Mahling, S.; Göbl, M.; Asmus, K.-D. *J. Am. Chem. Soc.* **1984**, *106*, 5382−5383.
(10) Asmus, K.-D.; Göbl, M.; Hiller, K.-O.; Mahling, S.; Mönig, J. *J. Chem. Soc., Perkin Trans.* **1985**, *2*, 641−646.
(11) Marciniak, B.; Bobrowski, K.; Hug, G. L.; Rozwadowski, J. *J. Phys. Chem.* **1994**, *98*, 4854−4860.
(12) Bobrowski, K.; Pogocki, D.; Schöneich, C. *J. Phys. Chem.* **1993**, *97*, 13677−13684.
(13) Bobrowski, K.; Pogocki, D.; Schöneich, C. *J. Phys. Chem. A* **1998**, *102*, 10512−10521.
(14) Marciniak, B.; Hug, G. L.; Rozwadowski, J.; Bobrowski, K. *J. Am. Chem. Soc.* **1995**, *117*, 127−134.
(15) Bobrowski, K.; Hug, G. L.; Marciniak, B.; Kozubek, H. *J. Phys. Chem.* **1994**, *98*, 537−544.
(16) Marciniak, B.; Bobrowski, K.; Hug, G. L. *J. Phys. Chem.* **1993**, *97*, 11937−11943.
(17) Bobrowski, K.; Marciniak, B.; Hug, G. L. *J. Am. Chem. Soc.* **1992**, *114*, 10279−10288.
(18) Steffen, L. K.; Glass, R. S.; Sabahi, M.; Wilson, G. S.; Schöneich, C.; Mahling, S.; Asmus, K.-D. *J. Am. Chem. Soc.* **1991**, *113*, 2141−2145.
(19) Hiller, K.-O.; Masloch, B.; Göbl, M.; Asmus, K.-D. *J. Am. Chem. Soc.* **1981**, *103*, 2734−2743.
(20) Bobrowski, K.; Holcman, J. *J. Phys. Chem.* **1989**, *93*, 6381−6387.
(21) Bobrowski, K.; Holcman, J. *Int. J. Radiat. Biol. Relat. Stud. Phys. Chem. Med.* **1987**, *52*, 139−144.
(22) Bobrowski, K.; Schöneich, C.; Holcman, J.; Asmus, K.-D. *J. Chem. Soc. Perkin Trans.* **1991**, *2*, 353−362.
(23) Bobrowski, K.; Schöneich, C. *Radiat. Phys. Chem.* **1996**, *47*, 507−510.
(24) Schöneich, C.; Yang, J. *J. Chem. Soc. Perkin Trans.* **1996**, *2*, 915−924.
(25) Schöneich, C.; Zhao, F.; Madden, K. P.; Bobrowski, K. *J. Am. Chem. Soc.* **1994**, *116*, 4641−4652.
(26) Bobrowski, K.; Schöneich, C.; Holcman, J.; Asmus, K.-D. *J. Chem. Soc., Perkin Trans.* **1991**, *2*, 975−980.
(27) Schöneich, C.; Pogocki, D.; Hug, G. L.; Bobrowski, K. *J. Am. Chem. Soc.* **2003**, *125*, 13700−13713.
(28) Schöneich, C.; Pogocki, D.; Wisniowski, P.; Hug, G. L.; Bobrowski, K. *J. Am. Chem. Soc.* **2000**, *122*, 10224−10225.
(29) Elango, N.; Janaki, S.; Rao, A. R. *Biochem. Biophys. Res. Commun.* **1978**, *83*, 1388−1395.
(30) Del Boccio, G.; Pennelli, A.; Whitehead, E. P.; Lo Bello, M.; Petruzzelli, R.; Federici, G.; Ricci, G. *J. Biol. Chem.* **1991**, *266*, 13777−13782.
(31) Jenei, Z.; Janaky, R.; Varga, V.; Saransaari, P.; Oja, S. S. *Neurochem. Res.* **1998**, *23*, 1085−1091.
(32) Hallier, E.; Deutschmann, S.; Reichel, S.; Bolt, H. M.; Peter, H. *Int. Arch. Occupat. Environ.* **1990**, *62*, 221−225.
(33) Peter, H.; Deutschmann, S.; Reichel, C.; Hallier, E. *Arch. Toxicol.* **1989**, *63*, 351−355.

Chart 1

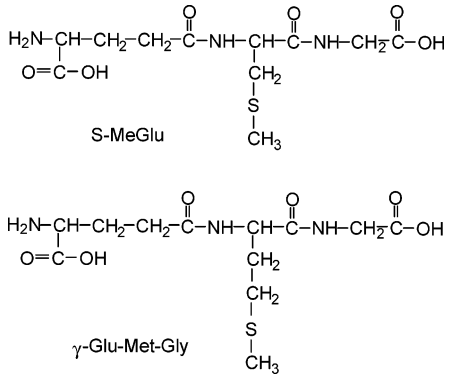

solutions purified by this procedure showed no anomalous transient absorptions at $\lambda = 360$ nm, indicative of sulfide radical cation−iodide interactions.[34]

The peptide γ-Glu-Met-Gly was synthesized by standard solid-phase methods using the Fmoc-protected amino acids. The peptide was characterized by FAB mass spectrometry, and its purity was checked by HPLC. The other chemicals were obtained as follows: perchloric acid ($HClO_4$) was purchased from Aldrich Chemical Co. (Milwaukee, WI), and reagent grade NaOH was obtained from T.J. Baker.

Solutions. All solutions were made with deionized water (18 MΩ resistance) provided by a Millipore MilliQ system. The pH was adjusted by the addition of either NaOH or $HClO_4$. Solutions were subsequently purged for at least 30 min per 500 mL of sample with the desired gas (N_2O or N_2) before pulse irradiation.

Pulse Radiolysis. Pulse radiolysis experiments were performed with the Notre Dame Titan 8 MeV Beta model TBS 8/16-1S linear accelerator with typical pulse lengths of 2.5−10 ns. A detailed description of the experimental setup has been given elsewhere along with the basic details of the equipment and the data collection system.[35] Absorbed doses per pulse were on the order of 2−10 Gy (1 Gy = 1 J kg^{-1}). Dosimetry was based on N_2O-saturated solutions containing 10^{-2} M KSCN, taking a radiation chemical yield of $G = 6.13$ (0.635 μM J^{-1}) and a molar extinction coefficient of 7580 M^{-1} cm^{-1} at 472 nm for the $(SCN)_2^{\bullet-}$ radical.[36] For practical purposes the *G*-unit rather than the SI-unit for radiation chemical yields is used throughout this paper. The *G*-unit denotes the number of species formed or converted per 100 eV of absorbed energy; $G = 1.0$ corresponds to 0.1036 μM per 1 J of absorbed energy in aqueous solutions.[37] Experiments were performed with a continuous flow of sample solutions at room temperature (∼23 °C). Experimental error limits are ±10% unless specifically noted.

Radiolysis of Water. Pulse irradiation of water leads to the formation of the primary reactive species shown in reaction 2.[37] In N_2O-saturated solutions ($[N_2O]_{sat} \approx 2 \times 10^{-2}$ M),[36] the hydrated electrons, e_{aq}^-, are converted into $^\bullet$OH radicals according to eq 3 ($k_3 = 9.1 \times 10^9$ M^{-1} s^{-1}).[36] Reaction 3 nearly doubles the amount of $^\bullet$OH radicals available for reactions with substrates.

$$H_2O \rightarrow {}^\bullet OH,\ e_{aq}^-,\ {}^\bullet H \qquad (2)$$

$$e_{aq}^- + N_2O \rightarrow O^{\bullet-} + N_2\ (+H_2O) \rightarrow {}^\bullet OH + OH^- + N_2 \qquad (3)$$

At pH < 4 the diffusion-controlled reaction of e_{aq}^- with protons becomes important (reaction 4, $k_4 = 2.0 \times 10^{10}$ M^{-1} s^{-1})[38] resulting in a pH-dependent lowered yield of $^\bullet$OH radicals and a correspondingly increased yield of $^\bullet$H atoms.

$$e_{aq}^- + H^+ \rightarrow {}^\bullet H \qquad (4)$$

The effective radiation chemical yields, *G*, of the primary species available for the reaction with a substrate depend on the concentration of the added substrate. For N_2O-saturated solutions, the effective radiation chemical yield of $^\bullet$OH radicals converting a given substrate into substrate-derived radicals can be calculated on the basis of the formula given by Schuler et al.[39] This formula relates the *G*-value of substrate radicals to the product k_s[S] of the rate constant for the reaction of $^\bullet$OH radicals with the substrate times the substrate concentration itself. For N_2-saturated solutions, the radiation chemical yield of $^\bullet$OH radicals was calculated based on a simple relationship which relates their yields with the scavenging capacity of the system.[40,41]

Molecular Modeling Details. The molecular modeling computations were performed for Met- and Cys(Me)-dipeptides [AcMetMe, AcCys(Me)Me], which served as models of the internal part of γ-Glu-Met-Gly and *S*-methylglutathione (*S*-MeGlu) peptides. All molecular mechanics (MM) simulations were performed in the extended atom model.[42] As potential energy function the CHARMM potential[43,44] in its HyperChem implementation was employed.[45] In order to simulate the presence of solvent (water), we utilized a scale factor (ϵ) equal to 80, which screened the charge−charge interactions. Such a simplification has been shown to give results that quantitatively agree with solvent simulations.[46] The modeling of nonoxidized peptides was done with the default Bio85+ set of parameters that is the equivalent of the PARAM19 parameter set,[47] augmented by parameters for the Met and Cys(Me) sulfur-centered cation-radicals obtained previously in ab initio calculations.[48] The statistical distribution of the distances separating the sulfur of Met or Cys(Me) from the oxygen of neighboring peptide bonds in model Met- and Cys(Me)-dipeptides was calculated by means of Langevin dynamics (LD)[42,49−54] without explicit solvent molecules and with a collision frequency (γ) for all heavy atoms equal to ∼50 ps^{-1}. The free LD simulations were done with a 2-fs time step and a 20-ns propagation time, preceded by 12 ps of heating from 0 to 300 K and an 18-ps equilibration. For the force-field calculations, we used version 7 of the HyperChem PC molecular modeling package,[55] which integrates the Langevin equation of motion using the method of Allen and Tildesley.[56]

Quantum mechanical (QM) calculations were performed for open-shell systems employing a commonly used, nonlocal hybrid functional,

(34) Hiller, K.-O.; Asmus, K.-D. *Int. J. Radiat. Biol.* **1981**, *40*, 583−595.
(35) Hug, G. L.; Wang, Y.; Schöneich, C.; Jiang, P.-Y.; Fessenden, R. W. *Radiat. Phys. Chem.* **1999**, *54*, 559−566.
(36) Janata, E.; Schuler, R. H. *J. Phys. Chem.* **1982**, *86*, 2078−2084.
(37) von Sonntag, C. *The Chemical Basis of Radiation Biology*; Taylor and Francis: New York, 1987.
(38) Buxton, G. V.; Greenstock, C. L.; Helman, W. P.; Ross, A. B. *J. Phys. Chem. Ref. Data* **1988**, *17*, 513−886.
(39) Schuler, R. H.; Hartzell, A. L.; Behar, B. *J. Phys. Chem.* **1981**, *85*, 192−199.
(40) LaVerne, J. A. *Radiat. Res.* **2000**, *153*, 196−200.
(41) LaVerne, J. A.; Pimblott, S. M. *J. Phys. Chem.* **1991**, *95*, 3196−3206.
(42) Leach, A. R. *Molecular Modelling: Principles and Applications*, 2nd ed.; Prentice Hall: Harlow, England, 2001.
(43) Brooks, B. R.; Bruccoleri, R. E.; Olafson, B. D.; States, D. J.; Swaminathan, S. K. M. *J. Comput. Chem.* **1983**, *4*, 187−217.
(44) Reiher, W. E. Harvard University, Cambridge, MA 1985.
(45) Molecular Mechanics. In *Hyperchem Computational Chemistry*; Hypercube, Inc.: Waterloo, Ontario, 1994; pp 139−185.
(46) Sneddon, S. F.; Brooks, C. L. I. *J. Am. Chem. Soc.* **1992**, *114*, 8220−8225.
(47) MacKarell, A. D. J. *PARAM19*, www.pharmacy.umab.edu/∼alex/research.html, 1999.
(48) Pogocki, D.; Schöneich, C. *Chem. Res. Toxicol.* **2002**, *15*, 408−418.
(49) Levy, R. M.; Karplus, M.; McCammon, J. A. *Chem. Phys. Lett.* **1979**, *65*, 4−11.
(50) Widmalm, G.; Pastor, R. W. *J. Chem. Soc., Faraday Trans.* **1992**, *88*, 1747−1754.
(51) Frenkel, D.; Smit, B. *Understanding Molecular Simulation: From Algorithms to Applications*, 2nd ed.; Academic Press: San Diego, 2002.
(52) He, S.; Scheraga, H. A. *J. Chem. Phys.* **1998**, *108*, 287−300.
(53) Field, M. J. *A Practical Introduction to the Simulation of Molecular Systems*; Cambridge University Press: Cambridge, 1999.
(54) Hinchlife, A. *Chemical Modelling: From Atoms to Liquids*; John Wiley & Sons: Chichester, UK, 1999.
(55) *HyperChem Computational Chemistry*; HyperCube Inc.: Waterloo, Ontario, Canada, 1996.
(56) Allen, M. P.; Tildesley, D. J. *Computer Simulation of Liquids*; Clarendon Press: Oxford, 1987.

B3LYP,[57] which appears to be particularly useful for the computation of optimized molecular geometries[58−61] and spin densities.[61−67] The DFT optimizations and energy calculations were performed utilizing the standard Gaussian 6-31+G(d) basis set.[68−70] (We have previously found that, for the $(S\therefore O)^+$-three-electron bonded systems, any further increase of basis set flexibility does not significantly change the resulting sulfur−oxygen bond lengths or the resulting unpaired spin densities on the sulfur and oxygen atoms.[71,72]) The 6-31+G(d) basis set includes diffuse and polarization functions on the heavy atoms only, and, as such, offers a compromise for the proper description of the anion-like species with good performance at a modest computational cost.[68,69,73,74] The radical structures were fully optimized using the analytical gradient technique, and the nature of each located stationary point was checked by evaluating harmonic frequencies. The vibrational frequencies (ω), obtained from conventional harmonic normal-mode analysis of the respective geometries, are shown without any corrections. To account for the effect of the solvent on the geometry of the radicals, the gas-phase structures were reoptimized in the integral equation formalism, solvent model (IEFPCM).[75−77] The theoretical estimates of the location of the dominating absorption bands (λ_{max}), an approximate description of absorption bands' intensities (electronic oscillator strength f), and the electronic nature of the transitions were obtained from time-dependent density functional response theory (TD-DFT).[78] The TD-DFT-B3LYP/6-311++G(d,p) calculations were done at the geometries obtained on the B3LYP/6-31+G(d) level. All the DFT calculations were performed with the Gaussian '98 suite of programs.[79] The input file structures of the radicals were prepared using the ISIS Draw 2.2.1 graphics program.[80] The visualization of the QM computation results and the molecular fitting[42] were done using the gOpenMol 2.1 program.[81] The file format conversions between modeling programs were done using the Babel 1.6 freeware program.[82]

(57) Becke, A. D. *J. Chem. Phys.* **1993**, *98*, 5648−5652.
(58) Bauschlicher, C. W., Jr.; Partridge, H. *Chem. Phys. Lett.* **1995**, *240*, 533−540.
(59) Carmichael, I. *Nukleonika* **2000**, *45*, 11−17.
(60) Zwier, J. M.; Wichers-Hoeth, J.; Brouwer, A. M. *J. Org. Chem.* **2001**, *66*, 466−473.
(61) Carmichael, I. *Acta Chem. Scand.* **1997**, *51*, 567−571.
(62) Carmichael, I. *J. Phys. Chem. A* **1997**, *101*, 4633−4636.
(63) Hug, G. L.; Carmichael, I.; Fessenden, R. W. *J. Chem. Soc., Perkin Trans.* **2000**, *2*, 907−908.
(64) Eriksson, L. A.; Malkina, O. L.; Malkin, V.; Salahub, D. R. *J. Chem. Phys.* **1994**, *100*, 5066−5075.
(65) Barone, V.; Adamo, C.; Russo, N. *Int. J. Quantum Chem.* **1994**, *52*, 963−971.
(66) O'Malley, P. J. *J. Comput. Chem.* **1999**, *20*, 1292−1298.
(67) O'Malley, P. J. *J. Phys. Chem. A* **1998**, *102*, 248−253.
(68) Davidson, E. R.; Feller, D. *Chem. Rev.* **1986**, *86*, 681−696.
(69) Labanowski, J. K. Simplified introduction to ab initio basis sets. terms and notation; www.chem.utas.edu.au/staff/yatesb/modules/mod5/jan_basis.html; Ohio Computer Center: Columbus, OH, ed. 2001.
(70) Jensen, F. *Introduction to Computational Chemistry*; John Wiley & Sons Ltd.: Chichester, 1999.
(71) Pogocki, D.; Schöneich, C. *J. Org. Chem.* **2002**, *67*, 1526−1535.
(72) Pogocki, D.; Serdiuk, K.; Schöneich, C. *J. Phys. Chem. A* **2003**, *107*, 7032−7042.
(73) Dunning, T. H., Jr.; Hay, P. J. *Modern Theoretical Chemistry*; Plenum Press: New York, 1997.
(74) Hehre, W. J. *Practical Strategies for Electronic Structure Calculations*; Wavefunction, Inc.: Irvine, CA, 1993.
(75) Cances, E.; Mennucci, B.; Tomasi, J. *J. Chem. Phys.* **1997**, *107*, 3032−3041.
(76) Cances, E.; Mennucci, B.; Tomasi, J. *J. Chem. Phys.* **1998**, *109*, 260−266.
(77) Cossi, M.; Barone, V.; Mennucci, B.; Tomasi, J. *Chem. Phys. Lett.* **1998**, *286*, 253−260.
(78) Casida, M. E.; Jamorski, C.; Casida, K. C.; Salahub, D. R. *J. Chem. Phys.* **1998**, *108*, 4439−4449.
(79) Pople, J. A.; et al. *Gaussian 98*, revision A.7; Gaussian Inc: Pittsburgh PA, 1998.
(80) *ISIS Draw 2.2.1*, http://www.mdli.com; MDL Information Systems Inc., 1999.
(81) Laaksonen, L. *gOpenMol 2.10*, http://laaksonen.csc.fi/gopenmol/gopenmol.html, 2001.
(82) Walters, P.; Stahl, M. *Babel 1.6.*, http://www.chem.ohiou.edu/~dolataa/babel.html, 1999.

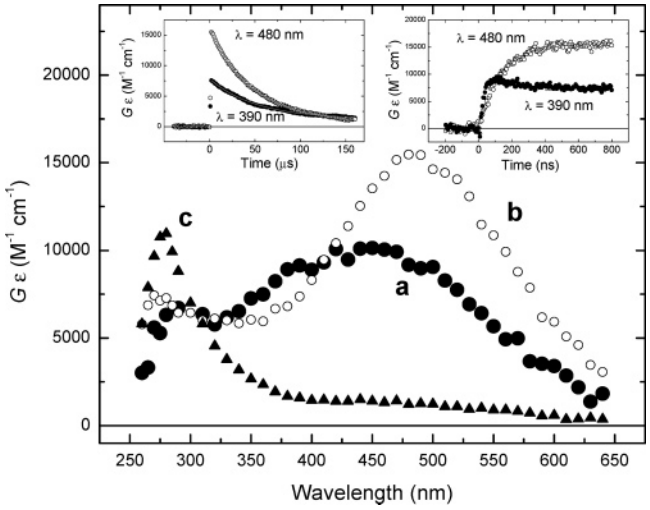

Figure 1. Absorption spectra recorded in N_2O-saturated aqueous solution containing 5 mM *S*-MeGlu at pH 1. Spectrum a, time delay 120 ns; spectrum b, time delay 700 ns; spectrum c, time delay 150 μs. Insets: time profiles representing growths (right) and decays (left) at $\lambda = 390$ and 480 nm.

Results and Discussion

The reaction of •OH radicals with *S*-MeGlu was investigated in both N_2O and N_2-saturated solutions of *S*-MeGlu over the concentration range of 0.1−5 mM, and at various pH values. Depending on the pH and the concentration of the solute, pulse irradiation leads to different transient optical spectra.

Absorption Spectra and Kinetics at Low pH. A transient spectrum, obtained 120 ns after the electron pulse in N_2O-saturated solutions containing 5 mM of *S*-MeGlu at pH 1, exhibits a broad absorption band in the 300−600 nm range with $\lambda_{max} = 450$ nm and a second, weaker UV absorption band with $\lambda_{max} = 290$ nm. The respective $G \times \epsilon$ values are $G \times \epsilon_{450} = 10{,}100\ M^{-1}\ cm^{-1}$ and $G \times \epsilon_{290} = 6700\ M^{-1}\ cm^{-1}$ (Figure 1, curve a). After ~700 ns, the transient absorption spectrum is dominated by the 480-nm band with $G \times \epsilon_{480} = 15{,}500\ M^{-1}\ cm^{-1}$ (Figure 1, curve b). This band decays within 150 μs after the pulse with $k_{obs} = 2.1 \times 10^4\ s^{-1}$, leaving a transient spectrum with a strong UV band having $\lambda_{max} = 280$ nm and $G \times \epsilon_{280} = 11{,}000\ M^{-1}\ cm^{-1}$ (Figure 1, curve c). For chemical reasons it was anticipated (and supported by findings described below) that the broad absorption spectrum with $\lambda_{max} = 450$ nm represents combined absorption bands of at least two different species. For example, the two kinetic traces, recorded at wavelengths 390 and 480 nm, are characterized by distinctly different time profiles (Figure 1, insets). On one hand the kinetic trace at $\lambda = 390$ nm reaches a plateau within 120 ns with $k_{obs}(\text{growth}) = 5.6 \times 10^7\ s^{-1}$. On the other hand, the kinetic trace at $\lambda = 480$ nm reaches a plateau within 700 ns with $k_{obs}(\text{growth}) = 7.5 \times 10^6\ s^{-1}$.

Figure 2 shows that the transient spectra were very sensitive to the concentration of *S*-MeGlu. Therefore, for better comparisons, all spectra were recorded in time windows after both the 390-nm and 480-nm traces reached their respective plateaus for each concentration of *S*-MeGlu. For 2 mM *S*-MeGlu, under the same conditions as above, the spectrum recorded 200 ns after the pulse consisted of an intense band with $\lambda_{max} = 400$ nm and $G \times \epsilon_{400} = 9300\ M^{-1}\ cm^{-1}$. It is important to note that this band contains two shoulders, one on the UV side and a second one in the neighborhood of 480 nm (Figure 2A, curve

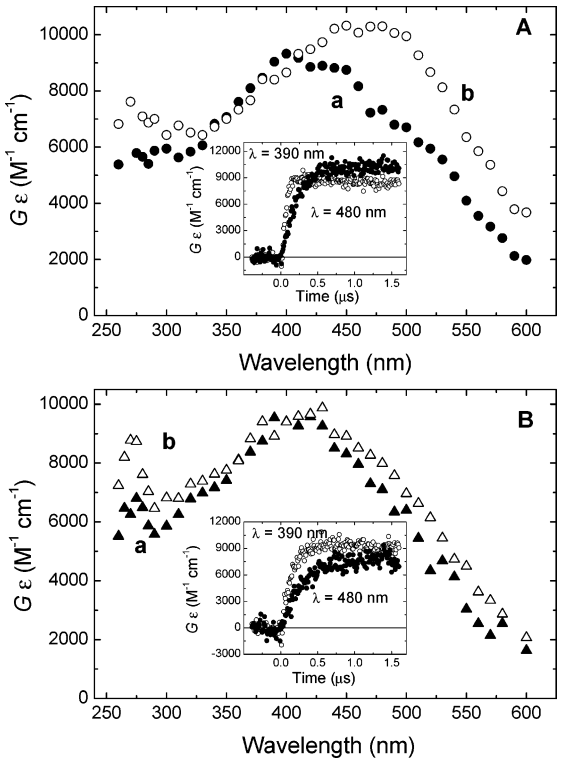

Figure 2. Absorption spectra recorded in N_2O-saturated aqueous solutions at pH 1. (Panel A) *S*-MeGlu (2 mM), curve a, time delay 200 ns; curve b, time delay 1.4 μs; (panel B) *S*-MeGlu (1 mM), curve a, time delay 500 ns; curve b, time delay 1.3 μs. (Insets in panels A and B) Time profiles representing growths at $\lambda = 390$ and 480 nm.

a). The latter shoulder became more pronounced 1.4 μs after the pulse and developed into a broad spectrum with $\lambda_{max} = 480$ nm and $G \times \epsilon_{480} = 10{,}300$ M^{-1} cm^{-1} (Figure 2A, curve b).

When the *S*-MeGlu concentration was further decreased to 1 mM, the spectrum, recorded 500 ns after the pulse, exhibited a broad absorption spectrum in the 300−600 nm range with $\lambda_{max} = 390$ nm. For these bands the respective radiation chemical yields amounted to $G \times \epsilon_{390} = 9800$ M^{-1} cm^{-1} and $G \times \epsilon_{480} = 7700$ M^{-1} cm^{-1} (Figure 2B, curve a). There was also a weak second UV absorption band with $\lambda_{max} = 270$ nm. A transient absorption band, present 1.3 μs after the pulse, exhibited a similar broad spectrum. However, it shifted to longer wavelengths with $\lambda_{max} = 430$ nm and $G \times \epsilon_{430} = 9650$ M^{-1} cm^{-1} (Figure 2B, curve b).

It is noteworthy that for the latter concentration (1 mM), a broad absorption band with $\lambda_{max} = 480$ nm did not develop even at longer time scales. However, the 390- and 480-nm kinetic traces recorded in solutions containing 1 and 2 mM *S*-MeGlu (Figure 2, insets) were characterized by distinctly different time profiles, analogous to the behavior observed in solutions of 5 mM S-MeGlu. On one hand, for example, the kinetic traces at $\lambda = 390$ nm reached plateaus within 200 ns with k_{obs}(growth) $= 2.4 \times 10^7$ s^{-1} in solutions of 2 mM *S*-MeGlu (Figure 2A, inset), and within 600 ns with k_{obs}(growth) $= 7.2 \times 10^6$ s^{-1} in solutions of 1 mM *S*-MeGlu (Figure 2B, inset). On the other hand, the kinetic traces at $\lambda = 480$ nm reached plateaus within 1.0 μs with k_{obs}(growth) $= 4.6 \times 10^6$ s^{-1} in solutions of 2 mM *S*-MeGlu (Figure 2A, inset), and within 1.4 μs with k_{obs}(growth) $= 3.4 \times 10^6$ s^{-1} in solutions of 1 mM *S*-MeGlu (Figure 2B, inset). This behavior can be rationalized by the existence of at least two distinct species, where the

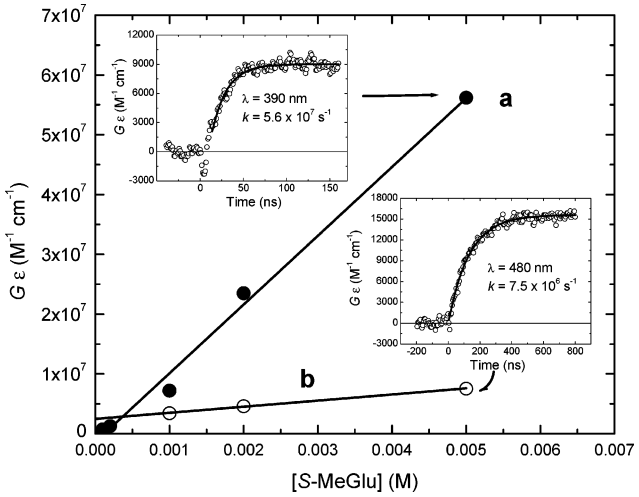

Figure 3. Pseudo-first-order growth plots of 390-nm kinetic traces (curve a) and 480-nm kinetic traces (curve b) for *S*-MeGlu in N_2O-saturated aqueous solutions at pH 1. (Insets) Kinetic traces recorded at $\lambda = 390$ nm (left) and $\lambda = 480$ nm (right) and their least-squares fits to first-order growths.

formation of one of them (characterized by the 480-nm band) is facilitated by high concentrations of *S*-MeGlu.

By analogy to other thioether systems,[4,7,13,19,83−86] where the intensities and half-lives of their transient 480-nm bands increase with increased [*S*-MeGlu], the 480-nm absorption band is assigned to the intermolecularly S∴S-bonded radical cations formed in reactions 5−7.

$$^{\bullet}OH + S\text{-MeGlu} \rightarrow S\text{-MeGlu}(>S^{\bullet}-OH) \quad (5)$$

$$S\text{-MeGlu}(>S^{\bullet}-OH) + H^+ \rightarrow S\text{-MeGlu}(>S^{\bullet+}) + H_2O \quad (6)$$

$$S\text{-MeGlu}(>S^{\bullet+}) + S\text{-MeGlu} \rightarrow S\text{-MeGlu}(>S\therefore S<)^+ \quad (7)$$

At this point in the exposition, we will not attempt to assign definitively the species responsible for the 390-nm absorption band. However, we note that this absorption band is formed at low *S*-MeGlu concentration and that its λ_{max} is similar to transient λ_{max}'s observed for various thioethers having neighboring carboxylate,[8−10,18,20,21,25] amide,[5] and hydroxyl groups.[6−9] This correspondence between λ_{max} and groups containing oxygen strongly suggests the existence of an intramolecularly $(S\therefore O)^+$-bonded species.

An additional interesting feature concerns the quantification of the rate constants for the formation of the 390- and 480-nm bands. The plots of k_{obs} (390/480) against [*S*-MeGlu] show good straight lines with the slopes representing the respective bimolecular rate constants for the formation of the intramolecularly $(S\therefore O)^+$-bonded species (k_{390}) (Figure 3, curve a) and the intermolecularly S∴S-bonded radical cations (k_{480}) (Figure 3, curve b).

The bimolecular rate constant $k_{390} = 1.2 \times 10^{10}$ M^{-1} s^{-1} was computed from the slope of curve a in Figure 3. Since the

(83) Asmus, K.-D. *Nukleonika* **2000**, *45*, 3−10.
(84) Chaudhri, S. A.; Mohan, H.; Anklam, E.; Asmus, K.-D. *J. Chem. Soc., Perkin Trans.* **1996**, *2*, 383−390.
(85) Asmus, K.-D. Sulfur-centered three-electron bonded radical species. In *Sulfur-Centered Reactive Intermediates in Chemistry and Biology*; Chatgilialoglu, C., Asmus, K.-D., Eds.; Plenum Press: New York, 1990; Vol. 197, pp 155−172.
(86) Bonifacic, M.; Möckel, H.; Bahnemann, D.; Asmus, K.-D. *J. Chem. Soc., Perkin Trans.* **1975**, *2*, 675−685.

plot of k_{obs} (390) vs [*S*-MeGlu] does not show departure from the linearity (Figure 3, curve a) and since the decay (reaction 6) of the initially formed hydroxysulfuranyl radicals of *S*-MeGlu (in reaction 5) is expected to be very fast at high proton concentrations, the formation rate constant of the 390-nm intermediate (k_{390}) corresponds to the rate constant for the reaction of $^{\bullet}$OH radicals with *S*-MeGlu (k_5). For this to be consistent with the above tentative assignment of the 390-nm band to the $(S\therefore O)^+$-bonded species, the rate constant of the reaction 8 (k_8)

$$S\text{-MeGlu}(>S^{\bullet+}) \rightarrow S\text{-MeGlu}(>S\therefore O)^+ \qquad (8)$$

must be much faster than k_5[*S*-MeGlu]. This has to be true at least in the concentration range up to 5 mM *S*-MeGlu, thus setting the lower limit for $k_8 \geq 6 \times 10^7$ s^{-1}. This value does not differ much from the rate constant for the formation of the five-membered intramolecularly (S∴O)-bonded intermediate in (carboxyalkyl)thiopropionic acid derivatives.[13]

The bimolecular rate constant $k_{480} = 1.0 \times 10^9$ M^{-1} s^{-1} was computed from the slope of curve b in Figure 3. Since the plot of k_{obs} (480) vs [*S*-MeGlu] does not show departure from the linearity (Figure 3, curve b) and since the decay (reaction 6) of the initially formed hydroxysulfuranyl radicals of *S*-MeGlu (in reaction 5) is expected to be very fast at high proton concentrations, the formation rate constant of the 480-nm intermediate (k_{480}) should correspond to the rate constant of sulfur monomeric radical cations (*S*-MeGlu($>S^{\bullet+}$)) reacting with *S*-MeGlu (k_7). This interpretation is justifiable because the pseudo-first-order rate constant (k_5) × [*S*-MeGlu] is always higher than the pseudo-first-order rate constant (k_7) × [*S*-MeGlu] over the concentration range (1−5 mM). The k_7 value fits very well into the range of values found for similar reactions in other thioether systems.[87−89]

Since the rate-determining step of the formation of $(S\therefore O)^+$-bonded species at pH 1 is the rate of the formation of *S*-MeGlu-($>S^{\bullet}-OH$) radicals in reaction 5 and since this rate is more than 1 order of magnitude faster than the rate of formation of intermolecularly S∴S-bonded radical cations in reaction 7, one would expect that the spectrum obtained at relatively low concentrations of *S*-MeGlu would not have contributions from *S*-MeGlu$(>S\therefore S<)^+$ radical cations. This hypothesis was checked as follows. A solution of low pH (acidified to pH = 1) was used so that reaction 6 would not be the rate-determining step in the formation of *S*-MeGlu($>S^{\bullet+}$). Furthermore, these conditions were employed in order to limit the involvement of the *S*-MeGlu($>S^{\bullet}-OH$) radicals in the formation of both *S*-MeGlu$(>S\therefore O)^+$ and *S*-MeGlu$(>S\therefore S<)^+$. Under these specific experimental conditions (pH 1, 0.1 mM *S*-MeGlu), the radiation−chemical yield of scavenged hydroxyl radicals is expected to be 2.5. The molar absorption coefficient (ϵ_{390}) for the $(S\therefore O)^+$-bonded species of *S*-MeGlu was calculated on the basis of this yield (vide infra).

The resulting transient spectrum, obtained 3.5 μs after the electron pulse in N_2O-saturated solutions containing 0.1 mM of *S*-MeGlu at pH 1, was dominated by the 390-nm band with $G \times \epsilon_{390} = 7500$ M^{-1} cm^{-1} and a second, weaker UV absorption band with $\lambda_{max} = 275$ nm and $G \times \epsilon_{275} = 5700$ M^{-1} cm^{-1} (Figure 4). Furthermore, contrary to the more concentrated *S*-MeGlu solutions (1−5 mM), the normalized kinetic traces recorded at the two wavelengths (390 and 480 nm) were characterized by identical time profiles. Both kinetic traces reached plateaus within 3.5 μs with k_{obs}(growth) = 7.1×10^5 s^{-1} (Figure 4, lower inset). As anticipated for chemical reasons (vide supra), the absorption band with $\lambda_{max} = 390$ nm can be assigned to the $(S\therefore O)^+$-bonded species without any contribution from intermolecularly bonded *S*-MeGlu$(>S\therefore S<)^+$ radical cations. This band decays within 150 μs after the pulse with $k_{obs} = 3.1 \times 10^4$ s^{-1} (Figure 4, upper inset). The ϵ_{390} value computed to be equal to 3000 M^{-1} cm^{-1} fits very well into the range of values found for similar (S∴O)-bonded species in other thioether systems having neighboring carboxylate,[8−10,18,20,21,25] amide,[27,28] and hydroxyl groups.[6−9]

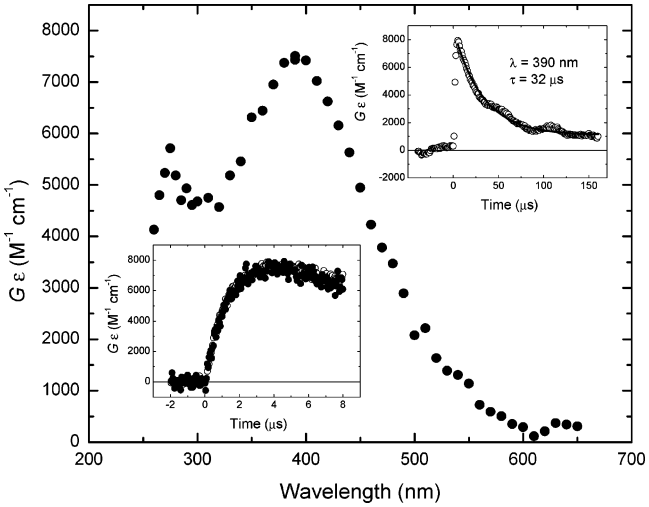

Figure 4. Absorption spectrum recorded 3.5 μs after the pulse in N_2O-saturated aqueous solution containing 0.1 mM of *S*-MeGlu at pH 1. (Insets) Time profiles representing growths at $\lambda = 390$ and 480 nm (lower); kinetic trace recorded at $\lambda = 390$ nm and its least-squares fit to the first-order decay (upper).

It should be noted that since experiments were carried out in very acid solutions, where most of the hydrated electrons are converted into $^{\bullet}$H atoms (reaction 4), the absorption in the UV region can be attributed to α-(alkylthio)alkyl radicals formed in *S*-alkylglutathiones through hydrogen abstraction by $^{\bullet}$H atoms.

$$^{\bullet}H + S\text{-MeGlu} \rightarrow S\text{-MeGlu}(-S-{}^{\bullet}CH_2) + H_2 \qquad (9)$$

Absorption Spectra and Kinetics at Neutral pH. The pulse irradiation of an N_2O-saturated solution, pH 6.4, containing 5 mM *S*-MeGlu led to the formation of a transient spectrum with $\lambda_{max} = 340$ nm and $G \times \epsilon_{340} = 11{,}000$ M^{-1} cm^{-1} (Figure 5, curve a).

This suggests, by analogy to similar findings for carboxyalkyl-sulfides,[12,13] that there is a contribution from a hydroxysulfuranyl radical ($>S^{\bullet}-OH$) which at 50 ns after the pulse has not yet converted into other transients. Figure 5 (curve b) shows that ($>S^{\bullet}-OH$) converts rapidly into a 390-nm absorption band, and by a slower process, ($>S^{\bullet}-OH$) transforms into another species with a 480-nm absorption band (Figure 5, curve c). The 480-nm absorption band is assigned to the intermolecularly S∴S-bonded radical cations.

The transient absorption spectra recorded at times greater than 350 ns exhibited an additional intense absorption band with λ_{max}

(87) Janata, E.; Veltwisch, D.; Asmus, K.-D. *Radiat. Phys. Chem.* **1980**, *16*, 43−49.
(88) Asmus, K.-D.; Bahnemann, D.; Fischer, C.-H.; Veltwisch, D. *J. Am. Chem. Soc.* **1979**, *101*, 5322−5329.
(89) Asmus, K.-D.; Bahnemann, D.; Bonifacic, M.; Gillis, H. A. *Faraday Discuss. Chem. Soc.* **1978**, *63*, 213−225.

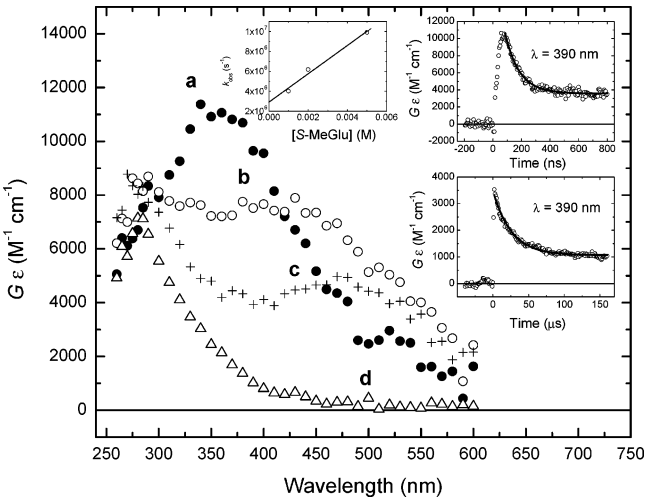

Figure 5. Absorption spectra recorded in N_2O-saturated aqueous solutions containing 5 mM of *S*-MeGlu at pH ≈ 6.5. Time delays of transient spectra: curve a, 50 ns; curve b, 140 ns; curve c, 350 ns, curve d, 150 μs. (Insets) Kinetic trace recorded at $\lambda = 390$ nm representing fast decay and its least-squares fit to the first-order decay (upper right); kinetic trace recorded at $\lambda = 390$ nm representing slow decay (lower); pseudo-first-order fits to decays analogous to that in the upper right inset (upper left).

$= 280$ nm ($G \times \epsilon_{280} = 7100$ M^{-1} cm^{-1}; Figure 5, curve d). This absorption band can be assigned (vide infra) to the combined absorption bands of α-(alkylthio)alkyl radicals and α-amino-type radicals. On one hand the α-(alkylthio)alkyl radicals could originate from the deprotonation of any initially formed intermolecularly S∴S-bonded radical cations (via the equilibrium with the sulfur monomeric radical cations $>S^{\bullet+}$, see below). On the other hand, the α-amino-type radicals are products of a decarboxylation process. The spectrum of α-amino radicals is characterized by a broad nondescript absorption band with no distinct λ_{max} at wavelengths >255 nm. The contribution of α-amino radicals to the spectrum in the wavelength region between 255 and 290 nm can be estimated by removing the more characteristic absorption spectrum of the α-(alkylthio)-alkyl radicals. A model for the absorption band of α-(alkylthio)-alkyl radicals can be found by looking at the •OH-induced oxidation of 2-(methylthio)ethanol since this reaction leads to the exclusive formation of α-(alkylthio)alkyl radicals.[7] This thioether derivative can then serve as a reference for the spectrum of α-(alkylthio)alkyl radicals formed in *S*-MeGlu. The UV spectrum of the α-(alkylthio)alkyl radical from 2-(methylthio)ethanol exhibits a characteristic 285-nm band which sharply decreases on both sides of the maximum. This band is also characterized by a ratio, $r = (\epsilon_{285}/\epsilon_{260}) \approx 2.0$. In contrast, this ratio is much lower in the spectrum recorded 150 μs after pulsed irradiation of the solution containing 5 mM *S*-MeGlu ($r \approx 1.4$; Figure 5, curve d). This indicates the presence of an additional shoulder in the 255−290 nm region. Evidence for α-amino-type radicals was confirmed earlier by monitoring their reduction of moderately good electron acceptors such as *p*-nitroacetophenone (PNAP) and methylviologen hydrate ($MV^{2+}\bullet H_2O$) in *S*-methylglutathione systems.[26]

Near neutral pH, the decay of the 390-nm absorption band showed biphasic kinetics, a feature that was not observed at pH 1. At pH 6.4, the 390-nm kinetic trace displayed a rapid decay with a half-life of $t_{1/2} = 70$ ns (Figure 5, upper right inset), followed by a slower decay with $t_{1/2} \approx 30$ μs (Figure 5, lower inset). The rate of the fast decay was found to be

Scheme 1

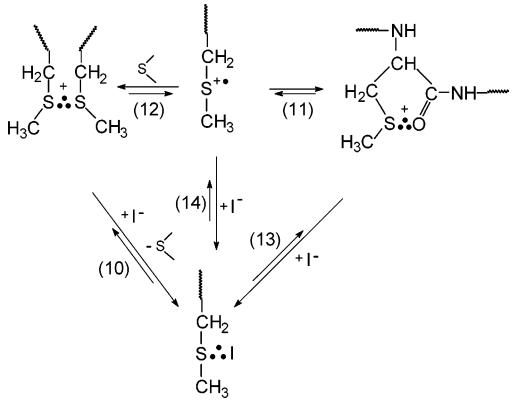

dependent on the *S*-MeGlu concentration (Figure 5, upper left inset). The slope of this plot gives the bimolecular rate constant, $k_{decay} = 1.4 \times 10^9$ M^{-1} s^{-1}, and the intercept of this plot yields the rate constant, $k_{incpt} = 2.9 \times 10^6$ s^{-1} (this value corresponds to $t_{1/2} = 240$ ns), for the *S*-MeGlu concentration-independent decomposition of the 390-nm short-lived transient. It was reported that a similar short-lived transient ($t_{1/2} \approx 320$ ns) is formed during the •OH-induced oxidation of threonylmethionine. This transient was assigned to a cyclic $[S\therefore NH_2]^+$-bonded species.[25] It is likely that the species responsible for the fast decay at 390 nm in the •OH-induced oxidation of *S*-MeGlu is a similar cyclic $[S\therefore NH_2]^+$-bonded species. The *S*-MeGlu concentration-independent decay of the $[S\therefore NH_2]^+$-bonded species leads to the parallel formation of CO_2 and α-aminoalkyl-type radicals. Evidence for the formation of this radical was seen in the buildup of an absorption at $\lambda = 270$ nm. The species responsible for the slow decay is most likely the intramolecularly $(S\therefore O)^+$-bonded species which is also observed at pH 1.

Quantification of $(S\therefore O)^+$-Bonded Species and Dimeric $(>S\therefore S<)^+$ Radical Cations. From the results presented so far, it can be seen that the transient spectra obtained at various pHs and *S*-MeGlu concentrations are actually superpositions of several absorption bands. It is necessary to resolve each of these composite spectra into their components in order to arrive at a quantitative description of the oxidation mechanism.

Since even low pH and high concentrations of *S*-MeGlu do not ensure the exclusive formation of dimeric intermolecularly S∴S-bonded radical cations, it is of interest to have a quantitative probe for their measurement. One possible probe is the reaction with iodide ions (reaction 10, Scheme 1).

Equilibrium 10 lies well on the side of the (>S∴I) complex since the latter complex is still present even at a [*S*-MeGlu]/$[I^-]$ concentration ratio of 500. This behavior is in accordance with similar findings in methionine[34] and aliphatic thioethers.[90] Equilibrium 10 was probed by monitoring the formation of the *S*-MeGlu(>S∴I) radical at 380 nm ($\epsilon_{380} = 7200$ M^{-1} cm^{-1})[34] as a function of time in N_2O-saturated solutions at two different pHs (1 and 6.2), containing various concentrations of *S*-MeGlu (1−5 mM) and I^- (0−40 μM). Close inspection of the 380-nm traces at pH 1 as a function of [*S*-MeGlu] reveals that the yield of *S*-MeGlu(>S∴I) radicals is almost constant and accounts for more than 80% of the •OH radicals. The comparable yield of *S*-MeGlu(>S∴I) radicals at a lower concentration of

(90) Bonifacic, M.; Asmus, K.-D. *J. Chem. Soc., Perkin Trans. 2* **1980**, 758−762.

S-MeGlu (1 mM) indicates that the reaction of iodide ions cannot be used as a reaction for probing exclusively *S*-MeGlu-$(>S\therefore S<)^+$ radical cations formed in reaction 7; however, I^- might also probe the *S*-MeGlu$(>S\therefore O)^+$ species as well via reaction 13 (Scheme 1). The *S*-MeGlu$(>S\therefore O)^+$ species are likely also in equilibrium with *S*-MeGlu$(>S\therefore S<)^+$ radical cations (equilibria 11 and 12, Scheme 1) and, therefore, will contribute to the reaction with I^- through equilibria 10 and 14 (Scheme 1).

The hypothesis that these two species exist in equilibrium is confirmed by two additional experimental observations. First, similar decay rate constants are measured at 390 and 480 nm (for example $k_d = 2.1 \times 10^4\ s^{-1}$ in 5 mM *S*-MeGlu) (Figure 1, inset), and second, both decay rate constants are affected in the same way on changing the *S*-MeGlu concentration (for example $k_d = 3.3 \times 10^4\ s^{-1}$ in 2 mM *S*-MeGlu).

Comparable yields of *S*-MeGlu$(>S\therefore I)$ radicals were also measured at various concentrations of *S*-MeGlu (1−5 mM) at pH 6.2; however, they are significantly lower than the *G*-values of *S*-MeGlu$(>S\therefore I)$ radicals measured at low pH. Their contribution constitutes only ∼15% of the available •OH radicals. These results are in accord with the efficient formation of $[S\therefore NH_2]^+$-bonded species which is expected on the basis of the high decarboxylation yields measured in this system.[26] In addition, because the yields of *S*-MeGlu$(>S\therefore I)$ radicals do not vary significantly over the investigated concentration range of *S*-MeGlu, this is an indication that at pH 6.2 both *S*-MeGlu-$(>S\therefore O)^+$ radicals and *S*-MeGlu$(>S\therefore S<)^+$ radical cations are formed with *S*-MeGlu$(>S\therefore O)^+$ likely dominating at low [*S*-MeGlu] and *S*-MeGlu$(>S\therefore S<)^+$ being more significant at high [*S*-MeGlu].

Influence of the Replacement of *S*-Methylcysteine by Methionine. The purpose of replacing the *S*-methylcysteine side chain in *S*-methylglutathione with methionine was to investigate the rate of the ring formations involving the $(S\therefore O)^+$-bond formation in the respective sulfur-centered radical cations. In *S*-MeGlu, there is only a single methylene group in the side chain of the central amino-acid residue as opposed to there being two methylene groups in the central amino-acid side chain in the tripeptide γ-Glu-Met-Gly. With *S*-MeGlu, it is possible to form five- or six-membered rings involving the sulfur radical cation bonding with the unpaired electrons of the oxygen atoms in the two peptide bonds on either side of it. However, with the extra methylene in the central side chain of γ-Glu-Met-Gly, only six- or seven-membered rings can be formed through bonding of the sulfur-centered radical cation with the unpaired electrons on the oxygen atoms of the adjacent peptide bonds.

The results can be seen in Figure 6. On one hand the transient spectrum following the •OH-induced oxidation of *S*-MeGlu showed a very intense band at 390 nm which is consistent with rapid formation of a five-membered $(S\therefore O)^+$-ring (Figure 6, curve a). On the other hand, the transient spectrum obtained on this same time scale following the •OH-induced oxidation of γ-Glu-Met-Gly exhibits a broad absorption spectrum in the 260−600 nm range with a very weak, broad absorption band, having $\lambda_{max} = 470$ nm ($G \times \epsilon_{470} = 800\ M^{-1}\ cm^{-1}$) and a stronger second UV absorption band with $\lambda_{max} = 280$ nm ($G \times \epsilon_{280} = 2200\ M^{-1}\ cm^{-1}$) (Figure 6, curve b). By analogy with *S*-MeGlu, the broad absorption band at $\lambda_{max} = 470$ nm might represent combined absorption bands of the six- or seven-membered $(S\therefore O)^+$-bonded species and the intermolecularly bonded γ-GluMetGly$(S\therefore S)^+$ dimeric radical cations. This latter observation indicates that the six- or seven-membered rings containing the $(S\therefore O)^+$ moiety do not form efficiently enough in order to be seen as a distinct absorption band in γ-Glu-Met-Gly. Further support for these conclusions is given in the molecular modeling results in the following section.

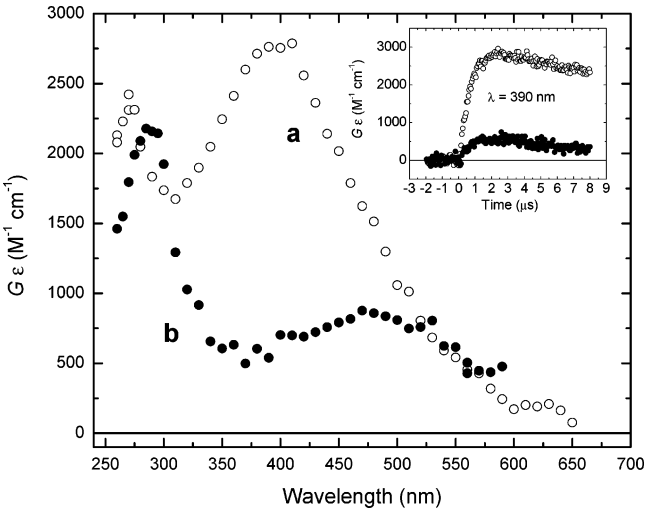

Figure 6. Transient absorption spectra recorded at 3 μs after the pulse in N_2O-saturated aqueous solutions at pH 1 containing 0.2 mM *S*-MeGlu (curve a) and γ-GluMetGly (curve b). (Inset) Kinetic traces recorded at $\lambda = 390$ nm in solutions containing *S*-MeGlu (open circles) and γ-GluMetGly (solid circles).

Even though Brunelle et al.[91] showed theoretical support for S∴N bonds coming from the oxidation of methionine side chains, such S∴N bonds are more likely to form at pH > 4. Thus, in the experiment shown in Figure 6, our assignment is that of an $(S\therefore O)^+$-bonded γ-Glu-Met-Gly species since the experiment was done at pH 1. The S∴N species are formed with a concurrent loss of OH^- from hydroxysulfuranyl radicals and a deprotonation of one of the amide nitrogens. At pH 1, loss of OH^- from the hydroxysulfuranyl radicals would most likely result via catalyzation via external protons.

Molecular Modeling Results

Distribution of the "$(S\therefore O)^+$-Bonded Conformers" in Model Cys(Me)- and Met-Dipeptides. The LD simulation shows that the investigated model Met- and Cys(Me)-dipeptides can adopt a certain number of conformations which may assist in the formation of intramolecular sulfur−oxygen bonds. The statistical distributions of the peptide conformers calculated in 20-ns LD simulations are presented in Figure 7.

During a 20-ns LD simulation, both peptides, the native one and the one-electron oxidized one, adopt conformations in which the thioether sulfur collides with the oxygen of one of the neighboring peptide functions. The average r_{S-O} is shorter than the sum of their van der Waals radii of the sulfur and oxygen atoms (∼3.32 Å).[92] Thus, in principle, the formation of an $(S\therefore O)^+$-bonded structure may be possible for the model Met-dipeptide as well as for the Cys(Me)-dipeptide.

On one hand a more detailed analysis of this qualitative picture shows a substantial probability for close contact between

(91) Brunelle, P.; Schöneich, C.; Rauk, A. *Can. J. Chem.* **2006**, *84*, 893−904.
(92) Bondi, A. J. *J. Phys. Chem.* **1964**, *68*, 441−451.

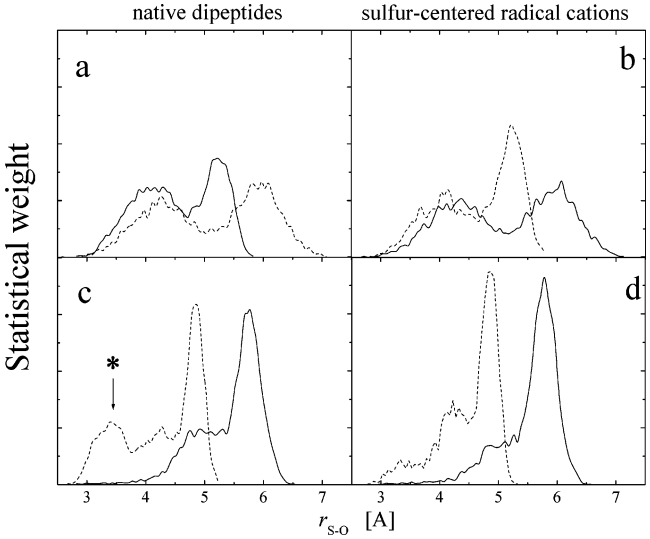

Figure 7. Statistical weights as a function of S−O distances from LD simulations. Dashed curves are for Cys(Me)-dipeptides, and solid curves are for Met-dipeptides. The r_{S-O} in panels a and b (c and d) refers the oxygen in the N-terminal (C-terminal) peptide moiety.

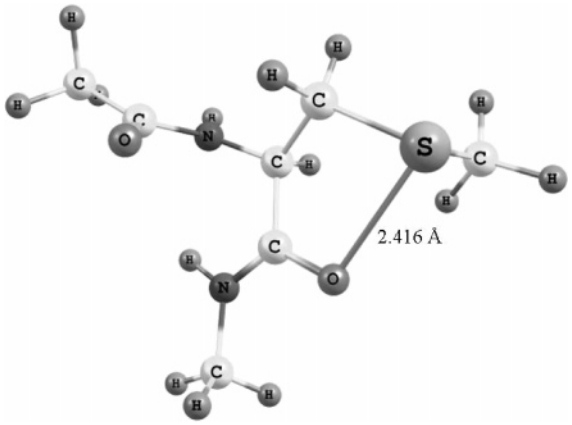

Figure 8. Optimized structure of the $(S\therefore O)^+$ radical cation of the Cys-(Me)-dipeptide.

the C-terminal peptide-bond oxygen and the thioether sulfur of the Cys(Me)-dipeptide and its cation radical. On the other hand, in the Met-dipeptide, the probability of close contact between the C-terminal peptide-bond oxygen and the thioether sulfur is very small. In contrast to this difference in the behavior at the C-terminal of the two dipeptides, there was no significant difference between the Cys(Me)- and the Met-dipeptides in regard to the distribution of distances between the thioether sulfur and the oxygen atom of the N-terminal peptide function.

Geometry and Spectral Properties of the $(S\therefore O)^+$-Bonded Radical Derived from Cys(Me)-Dipeptide. The geometry of the $(S\therefore O)^+$-bonded radical cation was fully optimized in the vicinity of the structure representing the conformer of the native Cys(Me) with $r_{(S-O)} \approx 3.3$ Å obtained from LD simulations. (That particular conformation is marked by a star in Figure 7c.) The gas-phase B3LYP/6-31+G(d) minimization of the $(S\therefore O)^+$-bonded radical cation leads to a stable conformer of the ^{3}E envelope form with $r_{(S-O)} = 2.416$ Å (see Figure 8).

The calculated vibrational frequency of the $(S\therefore O)^+$-bonded radical cation amounts to $\omega_{SO} = 557.6$ cm^{-1} ($F = 0.696$ N cm^{-1}), which can be assigned to the $(S\therefore O)^+$-bond stretch. The TD-DFT calculated energy of the most intense one-electron

Scheme 2

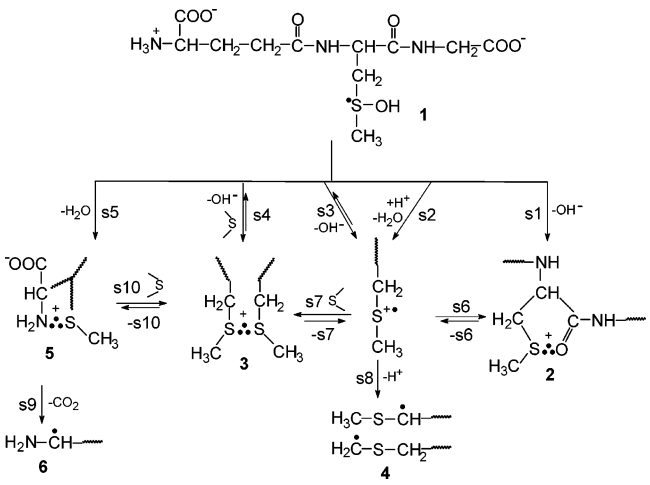

transition (3.1530 eV, 393.23 nm) fits well with the experiment for *S*-MeGlu. The calculated energy band is described essentially by an electronic transition from an occupied σ orbital of the $(S\therefore O)^+$-bond to a linear combination of mainly two σ^* molecular orbitals, as is evident from the weighting coefficient $c[\beta\rightarrow\beta^*] = 0.91$, see orbitals in Supporting Information.

Water-Phase Geometry. The IEFPCM($\epsilon = 78.4$) reoptimization of $(S\therefore O)^+$-bonded radical cation of Cys(Me) results in only a slight deformation of the gas-phase structure. (The rmsd of the Cartesian coordinates of atoms in this radical cation vs its solvated form is lower than 0.009 Å). In the previous works[71,72] we have shown a quasi-linear dependence of the $(S\therefore O)^+$-bond UV-absorption band on the bond length. Therefore, since taking into account the presence of water results only in an insignificant decrease of the $(S\therefore O)^+$-bond length ($\sim 1 \times 10^{-4}$ Å), we do not expect a significant solvent effect on the position of the calculated UV absorption band. Indeed the TD-B3LYP(IEFPCM)/6-311++G(d,p)//B3LYP(IEFPCM)/6-31+G-(d) calculated energy of the most intense (oscillator strength, $f = 0.1489$) one-electron transition (3.0500 eV, 406.5 nm) fits well with our prediction.[93]

Conclusions

Depending on the pH and the concentration of *S*-methylglutathione, •OH-induced oxidation of *S*-MeGlu leads to different transients. In order to rationalize these mechanistic differences, all the important reaction pathways are summarized in Scheme 2.

The initial reaction of •OH with *S*-methylglutathione is identical to those with simple aliphatic thioethers in that it leads to the formation of the hydroxysulfuranyl radical (**1**). However, substantial differences exist with respect to the subsequent reactions. At low pH values (i.e., 1.0), formation of the $(S\therefore O)^+$-bonded transient (**2**) can be rationalized by the sequence of reactions s2 and s6. The formation efficiency of intermolecularly bonded *S*-MeGlu$(>S\therefore S<)^+$ radical cations (**3**) depends on the concentration of *S*-MeGlu, and the reaction s7 accounts for that observation. Reaction s8 rationalizes the formation of α-(alkylthio)alkyl radicals (**4**) on longer time scales when both **2** and **3** decay. Of particular interest is a short-lived intermediate formed at higher pH values (6.4) that was assigned to the

(93) Pople, J. A.; et al. *Gaussian 03*, revision C.02; Gaussian, Inc.: Wallingford, CT, 2004.

intramolecularly bonded $[>S\therefore NH_2]^+$-radical cation (**5**). This transient is formed in a concerted process by which elimination of OH^- (in the form of water) involves a simultaneous deprotonation of the N-terminal $-NH_3^+$ group (reaction s5). It is worthwhile to note that the reactions s9 account for the fast decay of **5** that leads to the formation of α-amino radicals (**6**). Reaction s10 is postulated in order to accommodate the influence of *S*-MeGlu concentration on the decay of **5**. Since **2** and **3** are formed efficiently also at higher pH values, this observation suggests that reactions s1 and s4 represent important pathways for the formation of **2** and **3**, respectively. Molecular modeling was used to support the conclusions about the bonding associated with the ring formation of the sulfur-centered radical cations.

Acknowledgment. This work was supported by the Office of Basic Energy Sciences of the U.S. Department of Energy (Document No. NDRL-4720 from the Notre Dame Radiation Laboratory), the Polish Ministry of Scientific Research Grant (3 T09A 066 26), and ESF under COST Action P9 RADAM (KB and DP). The computation was performed employing the computing resources of the Interdisciplinary Centre for Mathematical and Computation Modelling, Warsaw University, Poland (G24-13, G28-21). G.L.H., B.M., and K.B. thank the NATO Collaborative Research Grants Program for a travel grant (Grant CRG973293).

Supporting Information Available: Complete refs 79 and 93; pictures of the orbitals involved in the $\sigma \rightarrow \sigma^*$ transition of the $(S\therefore O)^+$ radical cation. This material is available free of charge via the Internet at http://pubs.acs.org.

JA072301F